BENCHMARKING OF PATH AND RF-Track
IN THE SIMULATION OF LINAC4

G. Bellodi*, J.-B. Lallement, A. Latina, A. M. Lombardi, CERN, Geneva, Switzerland

Abstract

A benchmarking campaign has been initiated to compare PATH and RF-Track in modelling high-intensity, low-energy hadron beams. The development of extra functionalities in RF-Track was required to handle an unbunched beam from the source and to ease the user interface. The Linac4 RFQ and downstream accelerating structures were adopted as test case scenarios. This paper will give an overview of the results obtained so far and plans for future code development.

INTRODUCTION

RF-Track [1] is a tracking code developed at CERN for the optimization of low-energy ion linacs in the presence of space-charge effects. The code was initially created as a tool to perform tracking simulations of a medical linac for hadron therapy [2]; it then evolved to a multi-purpose accelerator toolbox capable of handling a large number of simulation scenarios [3]. RF-Track can simulate beams of particles with arbitrary energy, mass, and charge and transport them through conventional matrix-based elements as well as through field maps. It implements two different particle tracking methods: tracking in time and tracking in space. The first is preferred in space-charge-dominated regimes, where the relative positions of the particles in space matter.

The subject of this paper is the application of the RF-Track simulation capabilities to the case of low-energy, high-intensity hadron beams, such as the case of Linac4. For this purpose, a benchmarking campaign has recently started to compare RF-Track with the PATH [4] official simulation results, which were the reference for the design and commissioning of Linac4, showing extremely favourable comparisons with measurements . The use of RF-Track is motivated by the desire to extend the code's functionality to bridge the gap between electrons and ions while providing the Linac4 simulations with a modern code easily accessible through languages such as Octave and Python. As a first exercise, the RFQ and the Linac4 accelerating structures were adopted as test case scenarios, with the idea that the simulation should then be extended to cover from the source extraction at 45 keV to the final beam dump energy at 160 MeV.

MODELLING HIGH-INTENSITY LINACS

In a high-intensity linac the pulse length is typically much longer than the RF period . Nevertheless, after an initial transient, the beam dynamics on the scale of one RF period fully represents the behaviour of the whole pulse. The choice, in PATH, is to follow a section of the beam for as long as the

---

* giulia.bellodi@cern.ch

RF period . The flow of particles from one RF bucket to the adjacent one is correctly compensated for by longitudinal folding. In a high-intensity regime, RF-Track calculates the space-charge forces and integrates the equations of motion *in time*. If the beam is transported *in time*, folding is not possible. For this reason, we transported through the linac five full RF periods, assuming that the central one represents the steady state. This constitutes a significant difference between the simulation assumptions made by the two codes. PATH and RF-Track implement two very different space-charge calculation algorithms. In PATH, space-charge effects are calculated using the SCHEFF algorithm [5], which uses a 2D-rings-of-charge approximation, implicitly assuming cylindrical symmetry. The space around the beam ellipsoid is mapped in the laboratory frame with a radial and longitudinal mesh with user-defined step sizes. The electric self-field is then calculated in both components in the beam frame at each mesh vertex, assuming a uniform charge distribution on the mesh rings. The electric field at the coordinates of a particle P within the mesh is interpolated by the field values at the four adjacent mesh vertices. The force acting on the particle is finally transformed back to the laboratory frame.

In RF-Track, the space-charge kick is computed by solving the 3D Maxwell's equations for the electric-scalar and magnetic-vector potentials via a cloud-in-cell method based on integrated Green's functions. The kick on each particle is then computed as the Lorentz force due to the fields obtained from the electromagnetic potentials. No particular beam symmetry is here assumed.

As mentioned above, RF-Track tracks the 3D spatial distribution as it evolves *in time*. In PATH, the integration of the equations of motion is performed *in space*, and the spatial 3D distribution of the bunch is reconstructed at each space-charge kick.

RFQ

The Linac4 352.2 MHz RFQ was assumed as the first test case for benchmarking the two codes. The RFQ was described by a field map built out of FEM electrostatic simulations performed with COMSOL Multiphysics© [6], with the physical vane geometry taken into account to define the apertures. The stepsize of the field map was 0.2 mm. The file was directly imported in both PATH and RF-Track, and an initial beam distribution of 500 k macro-particles was used. Figures 1, 2, and 3 show the excellent agreement reached when tracking without space charge. The difference in overall transmission through the RFQ between the two codes is less than 0.5%, and the output beam distributions overlap very nicely in all three transverse and longitudinal phase spaces.
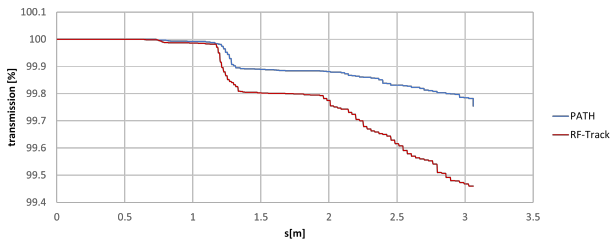
WEA3C2

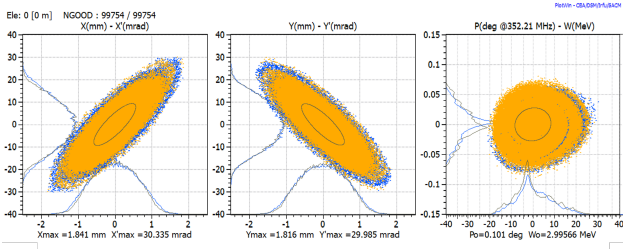Figure 1: Zero space charge transmission through the Linac4 RFQ.

Figure 2: Zero space charge RFQ beam output distribution in x-x′, y-y′, E-ϕ planes (left to right) for RF-Track (in blue) vs PATH (in yellow).
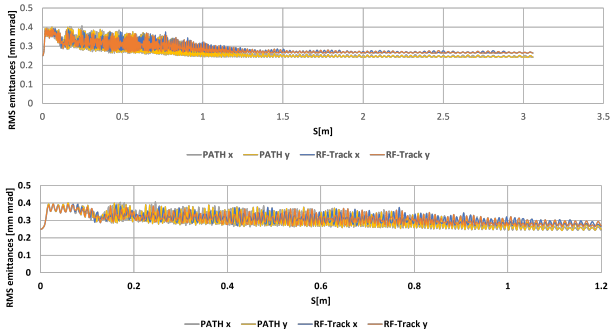

Figure 3: Zero space charge normalized RMS transverse emittances.

The benchmark became more complicated when one takes into account space-charge effects. In the RFQ beam dynamics tracking with PATH, the space charge model adopted is that for bunched beams, assuming 5 adjacent bunches for calculating the longitudinal repulsion (for DC beams, no longitudinal space charge forces would act in the longitudinal direction). Particles falling outside the 360-degree bucket during the bunching/accelerating process are automatically folded back into the bucket. This procedure is repeated at every calculation step until the end of the line. Such a feature is not yet implemented in the time-based RF-Track code. For the benchmarking purposes of this study, this option was therefore switched off in PATH simulations, and the space charge calculations were re-adjusted to match more closely the RF-Track approach (substituting the folding procedure with the tracking of an input beam extending longitudinally over five consecutive bunches and carrying five times the number of charges).

Figure 4 shows the transmission results for these different cases. The green curve was obtained by PATH standard simulations with 70 mA input beam current, bunched beam space charge model, and active folding option. The red curve was obtained with PATH when switching off the folding option and matching the RF-Track longitudinal space charge approach. The final discrepancy in transmission results of this latter case with RF-Track is below 4%. Figure 5 and Table 1 show the comparison of the output beam distributions in the transverse and longitudinal phase spaces.
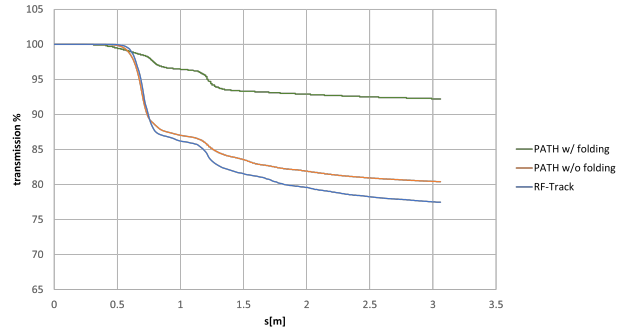

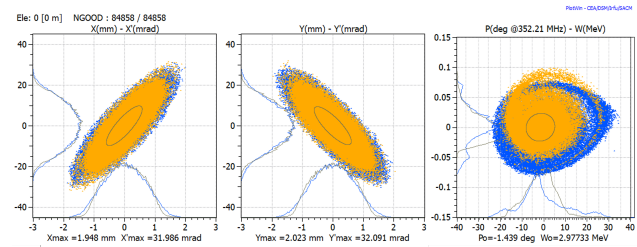Figure 4: RFQ transmission for 70 mA input beam current.

Figure 5: RFQ output beam distribution for 70 mA input beam current: PATH results are displayed in yellow, and RF-Track results in blue. The longitudinal plane in PATH simulations is obtained when switching off the folding option in the tracking.

Table 1: RFQ Output Beam Twiss Parameters

Parameter	PATH	RF-Track
Emittance x [mm mrad]	0.255	0.277
Beta x [m/rad]	0.109	0.118
Alpha x	-1.502	-1.602
Emittance y [mm mrad]	0.258	0.283
Beta y [m/rad]	0.115	0.120
Alpha y	1.461	1.524
Emittance z [deg MeV]	0.154	0.3
Beta z [deg/MeV]	286.062	338.886
Alpha z	-0.061	-0.127

LINAC4 CAVITIES

After the RFQ, the benchmarking studies focused on the beam dynamics in the Linac4 RF cavities. Linac4 is built

from three distinct accelerating structures: DTL, CCDTL, and PIMS, bringing the beam energy from 3 MeV to 50, 100 and 160 MeV, respectively. The DTL is composed of three cavities running at an accelerating field of 3.1 – 3.3 MV/m with an initial phase ramp. There are 39, 42 and 30 drift tubes per cavity. Every drift tube is different in dimensions and shape, and its length is adjusted to the velocity of the particles. For the beam dynamics production design of the DTL in both PATH and Tracewin [7], the DTL cavity is described as a sequence of drifts and zero-length RF gaps providing the acceleration kicks.
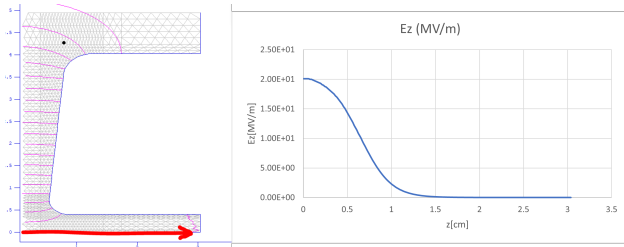

Figure 6: Longitudinal on-axis electric field in a DTL RF gap.

The benchmarking campaign was focused at this point on the comparison of the thin-gap model for particle acceleration used in PATH with a new approach, specially devised in RF-Track for this application, based on 1D field maps of the on-axis electric field obtained with Poisson-Superfish [8] (see Fig. 6). The shape of the longitudinal electric field in each RF gap is approximated with a generalized Gaussian distribution, whose main parameters are fitted case by case to reproduce the different gap geometry and the increasing gap length while matching the transit-time factor specified in the lattice file. The transverse electric field components are calculated from the derivatives of the on-axis field, with polynomial expansion extending to 3rd order [9, 10]. A hard edge model based on the 6D transfer matrix, is used to track through the quadrupoles. Figure 7 shows the RMS beam
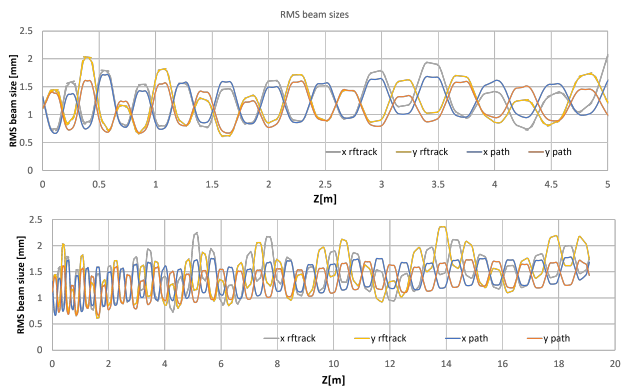

Figure 7: RMS beam size evolution along the DTL (bottom plot) and a zoomed-in version of the first few meters (top plot).

size evolution along the DTL as simulated by the two codes,
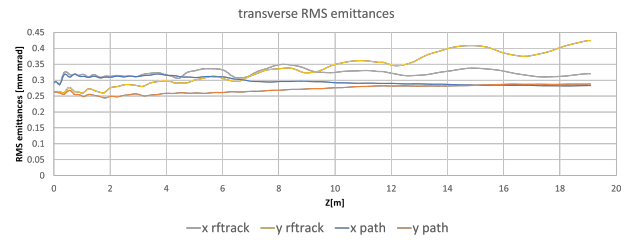

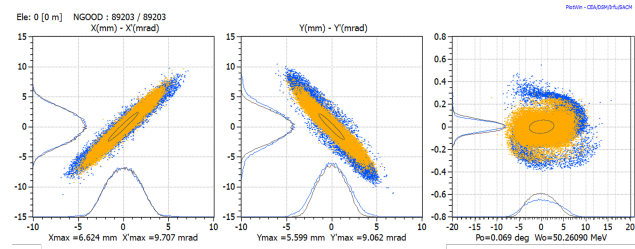Figure 8: Normalized RMS transverse emittances evolution along the DTL.

Figure 9: Output beam distribution at the end of the DTL in both transverse and longitudinal phase spaces. Path results are in yellow, and RF-Track results are in blue.

including space-charge effects. The difference between the two is mostly a few per cent. RF-Track results also present a "beating" pattern not observed in PATH, which we suspect is due to the different space-charge routines used in the two codes (as will be shown later). Figure 8 shows the RMS normalised transverse emittance evolution. Also, in this case, the agreement between simulation results is very good in the first few meters of the modelling, with the deviation growing in the end to about 10% in the horizontal plane and 40% in the vertical. This is also evident when looking at the final beam distribution in Fig. 9, showing a more important halo formation in the longitudinal plane for the RF-Track results and a slight mismatch in the vertical phase space. In contrast, a better agreement is obtained in the horizontal one. The Twiss parameters are listed for the two cases in Table 2.

Table 2: Output Beam Twiss Parameters

Parameter	PATH	RF-Track
Emittance x [mm mrad]	0.28	0.32
Beta x [m/rad]	3.22	3.18
Alpha x	-4.69	-4.21
Emittance y [mm mrad]	0.288	0.423
Beta y [m/rad]	2.37	2.31
Alpha y	3.45	3.88
Emittance z [deg MeV]	0.16	0.21
Beta z [deg/MeV]	47.34	51.69
Alpha z	-0.15	-0.45

Moving onwards from the Linac4 DTL, the benchmarking study was extended to cover beam dynamics tracking of the entire Linac4, with end-to-end simulations from 3 MeV to

160 MeV. The methods adopted were the same as described for the DTL, namely a thin RF gap model for PATH and a field map approximation model for RF-Track. As done for the modelling of the DTL RF gaps, the 1D field maps of the on-axis longitudinal electric field in the first CCDTL and PIMS cavities were used as input to a fitting procedure in RF-Track that, based on the detailed geometry of the structures, calculates and extracts *ad-hoc* the field in all downstream cavities to give the correct final beam acceleration.

DISCUSSION

Benchmarking results for zero space-charge trackings are very encouraging. Discrepancies in transverse emittance values are below 1% (see Fig. 10) and in RMS beam sizes, mostly below 10% (see Fig. 11). A comparison of the output beam distributions at 160 MeV is presented in Fig. 12, showing a fairly good agreement.
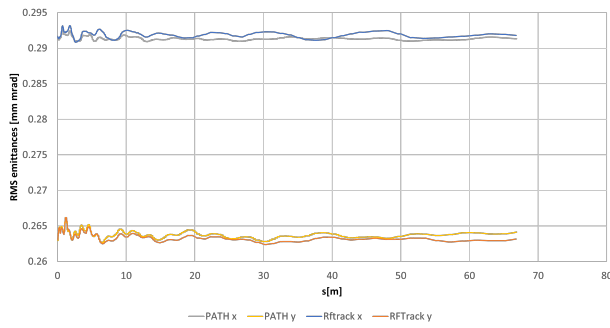

Figure 10: Horizontal and vertical RMS normalised emittances evolution along Linac4 (zero space charge).
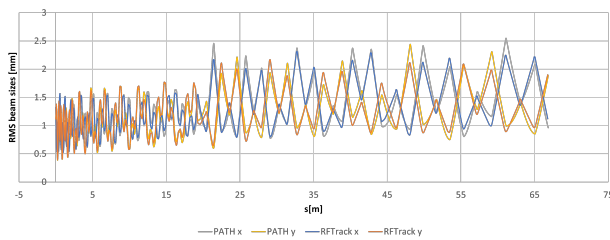

Figure 11: Horizontal and vertical RMS beam sizes along Linac4 (zero space charge)
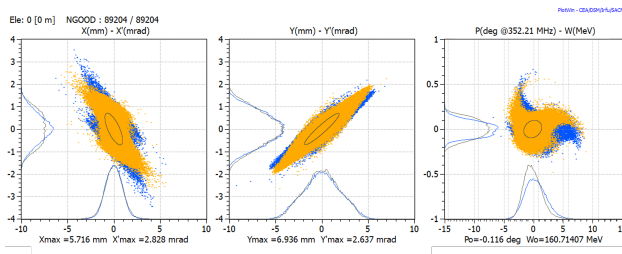

Figure 12: Zero space charge output beam distribution at PIMS exit. PATH results in yellow vs RF-Track results in blue.

Adding space charge to the simulations brought some differences in the results obtained with the two codes, especially impacting the transverse RMS emittances evolution, as already observed in the case of the DTL modelling alone (Fig. 8). This will require further work and understanding the details of the different beam dynamics models adopted in the two codes.

Besides the differences in the beam models simulated (folding or not) and the different space-charge models (SCHEFF or 3D), at least two more reasons can explain the differences visible in the phase space plots, e.g., Fig. 12:

1. PATH simulates the acceleration in DTL, CCDTL, and PIMS sections using thin kicks, whereas RF-Track uses 3D realistic field maps of all the RF elements in the lattice. In RF-Track, 46.8 meters of beamline out of 66.8 meters are constituted by realistic field maps (that is, 70.1% of the length).

2. PATH-generated energy curves have been used to set the phase and amplitude of the RF cavities, giving the correct energy and phase/energy spread at the PSB. The phase of each cavity has been set via beam-based measurements of the energy via time of flight measurement and compared with PATH/TRACEWIN prediction for the average beam energy. In RF-Track, the RF phases have been quickly tuned to achieve the desired energy gain but have yet to be optimised. For this reason, the phase advance through the system is not nominal, and the beam experiences an optics mismatch in each quadrupole that induces emittance growth.

CONCLUSION

A benchmarking of PATH and RF-Track beam dynamics tracking results in Linac4 has been kicked off, aiming to extend the realm of applicability of RF-Track to the simulation of low-energy, high-intensity beams. Adding new functionalities and *ad-hoc* procedures was required to model the adopted test cases of the Linac4 structures. In particular, a novel approach based on the approximation of the 1D field maps of the longitudinal on-axis electric field was chosen to be adopted in RF-Track instead of the more classical thin RF-gap model for beam acceleration used in PATH. The comparison of results obtained with zero space-charge tracking is very encouraging, and the discrepancies found are within a few per cent. Further understanding is needed, however, of the differences observed in the results when introducing space-charge effects. This issue may be clarified by testing different space charge setups available in RF-Track, based on time integration *vs* space integration modules, and by optimising the attribution of RF gap phases in RF-Track. Once the differences between the codes are smoothed out, and full validation is achieved, the next goal will be to complete the end-to-end modelling of Linac4 in RF-Track, including a proper simulation of the beam extraction from the source in a self-consistent time-based frame.

REFERENCES

[1] A. Latina, *RF-Track Reference Manual*, version 2.0.4, 2020. doi:10.5281/zenodo.4580369

[2] S. Benedetti, A. Grudiev, and A. Latina, "High gradient linac for proton therapy", *Phys. Rev. Accel. Beams*, vol. 20, p. 040 101, 4 2017. doi:10.1103/PhysRevAccelBeams.20.040101

[3] A. Latina, "Update of the RF-Track particle tracking code", in *Proc. IPAC'23*, Venice, Italy, May, 2023, pp. 3462–3465. doi:10.18429/JACoW-IPAC2023-WEPL151

[4] A. Perrin, J.-F. Amand, T. Mütze, and J.-B. Lallement, *Travel User Manual*, version 4.07, CERN, Geneva, Switzerland, Apr. 2007. https://lombarda.web.cern.ch/DTL-linac4/Travel.pdf

[5] "Multiparticle dynamics with space charge", in *RF Linear Accelerators*. 2008, ch. 9, pp. 282–340. doi:10.1002/9783527623426.ch9

[6] Multiphysics, COMSOL, "Introduction to COMSOL multiphysics®", 1998. https://cdn.comsol.com/doc/5.5/IntroductionToCOMSOLMultiphysics.pdf

[7] D. Uriot and N. Pichoff, *Tracewin documentation*, Université Paris-Saclay, Gif-sur-Yvette, France, updated Dec. 2021. https://irfu.cea.fr/dacm/logiciels/codesdacm/tracewin/tracewin.pdf

[8] *Reference manual for the POISSON/SUPERFISH Group of Codes*, Los Alamos National Laboratory, NM, USA, Rep. LA-UR-87-126, Apr. 1987. doi:10.2172/10140827

[9] T. Kamitani and L. Rinolfi, "Positron production at CLIC", CERN, Geneva, Switzerland, Rep. CERN-OPEN-2001-025, CLIC-Note-465, Oct. 2000. https://cds.cern.ch/record/492189/

[10] K. Flottman, *ASTRA User Manual*, DESY, Hamburg, Germany, Mar. 2017. http://www.desy.de/~mpyflo